ISSN 2075-1087, Gyroscopy and Navigation, 2017, Vol. 8, No. 1, pp. 43–50. © Pleiades Publishing, Ltd., 2017.
Original Russian Text © B.V. Klimkovich, A.M. Tolochko, 2016, published in Giroskopiya i Navigatsiya, 2016, No. 2, pp. 41–55.

A Correcting Filter for a Mechanically Dithered Single-Axis Ring Laser Gyro

B. V. Klimkovich* and A. M. Tolochko

Scientific Production Limited Liability Company OKB TSP, Minsk, Belarus

**e-mail: klimkovich_boris@mail.ru*

Received November 2, 2015

Abstract—A correcting digital filter for a mechanically dithered single-axis ring laser gyro (RLG) is proposed. The filter is intended to determine the angular position of a strapdown inertial navigation system (SINS) in the RLG sensitivity axis using the known value of the RLG angular position with respect to inertial space, taking into account the models of the suspension elastic forces nonlinearity, the hysteresis model of vibration energy dissipation, and the model of the suspension piezoceramic vibratory drive. Parameterized models of nonlinearity, dissipation, and the output characteristic of the suspension piezoceramic drive have been developed. A method for finding nonlinearity parameters of elastic forces using a set of experimental amplitude-frequency characteristics (AFC) is proposed. Numerical simulations of the AFCs of an elliptic eliminator and a correcting filter under sinusoidal rotation of the SINS with the amplitude of 1 arcmin in the frequency band of 80–3600 Hz have been performed. The efficiency of the proposed filter has been verified experimentally under pulse action on the SINS; the test results are discussed. Comparison of the experimental and calculated data shows the adequacy of the proposed models and satisfactory operation of the correcting digital filter.

DOI: 10.1134/S2075108716040064

INTRODUCTION

Ring laser gyroscopes (RLG) are widely employed in navigation-grade SINS [1–3]. RLG errors caused by lock-in of the counter-propagating modes at low speeds of rotation can be reduced due to nonreciprocal elements used in the external magnetic field or alternating-frequency mechanical dither [2, 3]. The latter technique makes RLG less sensitive to the magnetic field and provides higher accuracy of SINS. Application of alternating-frequency mechanical dither requires that the RLG body be installed on an elastic vibrosuspension (subsequently referred to as "suspension") with piezoceramic plates fixed to it. Under alternating voltage the suspension undergoes torsional vibrations in the RLG sensitivity axis [3, 9]. By these means, the RLG output signal contains a sum of the SINS angular position in a specified axis with respect to the inertial space and rotation of the RLG body with respect to the SINS. Only the first term is of importance for the inertial algorithm, whereas the RLG rotation due to dither should be excluded from the RLG output data. The electrodynamic method commonly used for this purpose suggests that a permanent magnet be fixed onto the RLG body and a coil, generating a voltage proportional to the RLG speed of rotation relative to the SINS, fixed onto the SINS body. The drawback of this method is significant time-and-temperature dependence of the coil analog signal and additional labor input in manufacturing.

Digital methods are currently in wide use for RLG signal processing. In this connection, various methods for mathematical elimination of dither from RLG signals have been developed in recent years [3–9]. A sequence of digitized RLG readings is passed through a narrowband digital filter, called an eliminator [3], adjusted to the RLG frequency of mechanical dither. However, this method has two significant drawbacks.

Firstly, complete suppression of frequencies in the vicinity of mechanical dither eliminates not only the dither but also the corresponding harmonics of the SINS rotation signal, giving rise to an error in the operation of the navigation algorithm.

Secondly, the inertial mass of the RLG body attached to the elastic suspension forms a mechanical oscillatory (rotary) loop, with the AFC decreasing inversely to the second power of the frequency for those above the resonance one. This means that, when used in the form presented in [3, 9], the eliminator limits the passband of the SINS rotational motion to the frequencies below the resonance one for the given suspension. Since the mechanical dither resonance frequencies for RLG with an optical path perimeter of 28 cm lie within the range between 300 and 450 Hz and are different for the three orthogonal axes of the SINS, the navigation algorithm operates on the data that are very limited in spectrum, which makes it impossible to correctly describe high-frequency components of the SINS rotational motion. At the same

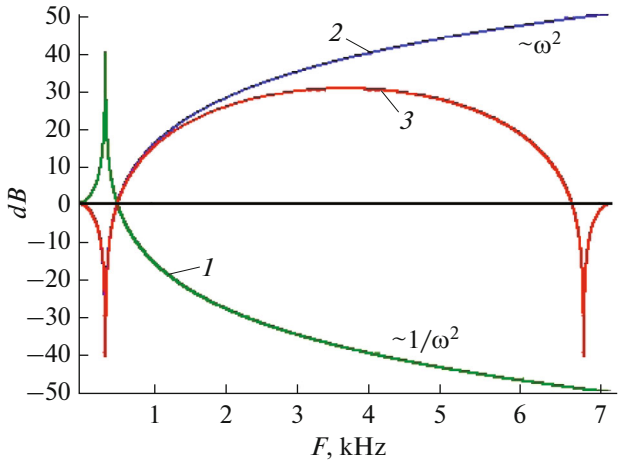

Fig. 1. AFC at the kinematic input of the oscillating system with damping (curve *1*; the dynamic input is not excited), AFC of the correcting analog filter (curve *2*), and AFC of the correcting digital filter (curve *3*, $\Delta T = 0.139$ ms).

time, currently the rotational motion passbands of modern navigation-grade SINS are no less than 1 kHz [10].

It is important that the above mentioned electrodynamic method is free from such drawbacks. At the same time, the idea of eliminating analog electronic components and replacing them with a mathematical algorithm is attractive. In this paper, the authors propose a digital filter designed for elimination of mechanical dither from the signal of a single-axis RLG.

CORRECTING FILTER

The proposed filter is intended to determine the SINS angular position φ_{SINS} with respect to the RLG sensitivity axis, provided that the angular position of the RLG body φ_{RLG} relative to the inertial coordinate system is known. Note that the case under consideration concerns a single-axis RLG.

The equation of the RLG body rotation by angle φ_{RLG} with the inertia moment I relative to the sensitivity axis under the action of the moment of forces M, taking into account the elasticity of the suspension, dissipation of oscillation energy, and the oscillations generated by the suspension piezoceramic plates with voltage V, can be written as

$$I\frac{d^2\varphi_{RLG}}{dt^2} = M \equiv M_{flex} + M_{diss} + M_{piezo}. \qquad (1)$$

Because of space isotropy, the moments of forces associated with elasticity M_{flex} and dissipation M_{diss} can only depend on the difference $\varphi_{RLG} - \varphi_{SINS}$, which makes it possible, after dividing the elastic forces into linear and nonlinear parts, to write Equation (1) as follows:

$$I\frac{d^2\varphi_{RLG}}{dt^2} = -c(\varphi_{RLG} - \varphi_{SINS} + \mathrm{Nonl}(\varphi_{RLG} - \varphi_{SINS}) + \mathrm{Diss}(\varphi_{RLG} - \varphi_{SINS}) + \mathrm{Piezo}(V)), \qquad (2)$$

where c is the suspension torsional rigidity, $\mathrm{Nonl}(\varphi_{RLG} - \varphi_{SINS})$ is the term describing nonlinearity of elastic forces, $\mathrm{Diss}(\varphi_{RLG} - \varphi_{SINS})$ is the term describing dissipation of oscillation energy, $\mathrm{Piezo}(V)$ is the term describing the moment of forces caused by the suspension piezoceramic plates.

Equation (2) describes an oscillation system with a combined—kinematic (φ_{SINS}) and dynamic ($\mathrm{Piezo}(V)$)—excitation [11].

It is known that the AFC of such a system at both excitation inputs is a resonance circuit, the quality factor of which is determined by losses $\mathrm{Diss}(\varphi_{RLG} - \varphi_{SINS})$.

Equation (2) can also be regarded as an equation of a mechanical filter, with φ_{SINS} at its input and φ_{RLG} at the output.

Because of the AFC ripple of the mechanical filter, the value φ_{RLG} measured by the RLG contains amplitude-and-phase distortions. At frequencies above the resonance one, AFC shows a roll-off of about $1/\omega^2$ (ω is an angular frequency), which is due to the second time derivative in the left side of Equation (2). The distortions can be corrected and dynamic excitation can be subtracted if the received signal φ_{RLG} is passed through an additional correcting filter, the AFC of which multiplied by the AFC of the mechanical filter in a required passband band should provide 1.

The correcting filter can be described by Equation (2) given above, but the input and output are reversed: φ_{RLG} is an input parameter, and the output parameter is, in the general case, the root of the nonlinear equation φ_{SINS}. At the frequencies above the resonance one, the AFC of the correcting filter shows the growth proportional to ω^2 (Fig. 1, curve *2*).

To obtain a correcting digital filter, we need to change over from the continuous (Equation (2)) to discrete time. For this purpose, taking into consideration the fact that the terms $\mathrm{Nonl}, \mathrm{Diss}, \mathrm{Piezo}$ are small (about ten arcsec), they are omitted in Equation (2) for the time being, whereby we derive:

$$\frac{1}{\omega_0^2}\frac{d^2\varphi_{RLG}}{dt^2} + \varphi_{RLG} = \varphi_{SINS}, \qquad (3)$$

where $\omega_0 = \sqrt{c/I}$ is the circular self-resonant frequency of the suspension at small oscillation amplitudes.

In the digital processing, the values of angles φ_{RLG} are available at discrete points in time with a sampling period of ΔT. To change over from the analog filter (3) to a discrete one, it is necessary, after the Laplace transformation and bringing the result to the canonical form, to make the following replacement in Equation (3):

$$s - p \to \frac{1 - z^{-1}e^{p\Delta T}}{\Delta T},$$

where s is the parameter of the Laplace transform, z is the parameter of Z-transformation, and p is the polynomial pole [12]. Therefore, after introducing the notations $X_n \equiv \varphi_{RLG}(t_n)$ and $Y_n \equiv \varphi_{SINS}(t_n)$, the equation of the digital filter takes the form:

$$Y_n = \frac{1}{(\omega_0\Delta T)^2}(X_n + X_{n-2} - 2X_{n-1}) + \frac{2(1-\cos(\omega_0\Delta T))}{(\omega_0\Delta T)^2}X_{n-1}. \quad (4)$$

After taking into account the terms Nonl, Diss, Piezo, we can finally write the formula for the correcting digital filter:

$$Y_n = \frac{1}{(\omega_0\Delta T)^2}(X_n + X_{n-2} - 2X_{n-1}) + \frac{2(1-\cos(\omega_0\Delta T))}{(\omega_0\Delta T)^2}(X_{n-1} + \mathrm{Nonl}(X_{n-1} - Y_{n-1}) + \mathrm{Diss}(X_{n-1} - Y_{n-1}) + \mathrm{Piezo}(V_{n-1})). \quad (5)$$

Equation (5) solves the problem of determining the SINS angular position φ_{SINS} in the RLG sensitivity axis, provided that the angular position of the RLG body φ_{RLG} relative to the inertial coordinate system in digital form is known and the functional dependences of Nonl, Diss, Piezo on their arguments are also known.

Note that the AFC of the correcting digital filter shows lower values in the Nyquist frequency band $F_N = 1/2\Delta T$ as compared with the AFC of the corresponding analog filter due to the symmetry of the AFC of the correcting filter with respect to the specified frequency (Fig. 1, curve *3*) and quadratic dependence of the AFC of the correcting analog filter on the frequencies above the resonance one.

The accuracy of the angular position φ_{SINS} provided by the correcting digital filter (5) depends on the accuracy of parameters obtained for the corresponding mechanical filter of the suspension. Therefore, in order to use filter (5) in practice, it is necessary to represent the dependencies Nonl, Diss, Piezo in the form of parameterized functions. Because of the temperature and time dependence of the resonance frequency ω_0 and the parameters of functions Nonl, Diss, Piezo, the latter should be estimated and corrected in the operation mode of the SINS.

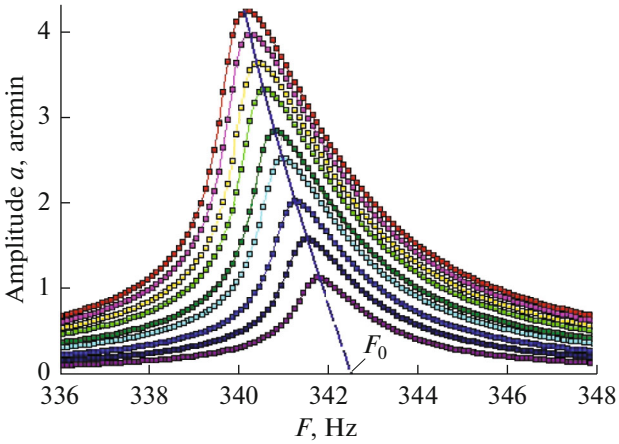

Fig. 2. Oscillation amplitude of an RLG with a perimeter of 28 cm at dynamic excitation.

NONLINEARITY OF ELASTIC FORCE

To specify the dependence Nonl(φ), we consider the experimental oscillation amplitude dependences of the RLG suspension on the frequency. The RLG with a 28 cm perimeter was subjected to dynamic excitation with fixed amplitudes of ac voltage V. Figure 2 shows an example of such dependencies.

Two specific features of the AFC set of the elastic suspension are the following: decrease of the resonance frequency with the increase of the amplitude, and asymmetry of the resonance curve. The values of asymmetry of the resonance curves may vary for RLGs from different manufacturers.

To determine the function Nonl(φ) from the experimental dependence of the period of resonance oscillations $T(E)$ on oscillation energy E, we can use the known formula (12.2) [13] for single-axis rotation of a body with the moment of inertia I:

$$\varphi(U) = \frac{1}{2\pi\sqrt{2I}}\int_0^U \frac{T(E)dE}{\sqrt{U-E}}. \quad (6)$$

Introducing variable amplitudes of oscillation a and integration parameter v, using the definitions $U \equiv \frac{ca^2}{2}$ and $E \equiv \frac{cv^2}{2}$, we can go from integration with respect to energy E to integration with respect to oscillation amplitude; thus, from Equation (6) we derive:

$$\varphi(a) = F_0\int_0^a \frac{v\,dv}{F(v)\sqrt{a^2 - v^2}}, \quad (7)$$

where F_0 is the resonance frequency at small oscillations (see Fig. 2), $F(v)$ is the dependence of the resonance frequency on the oscillation amplitude.

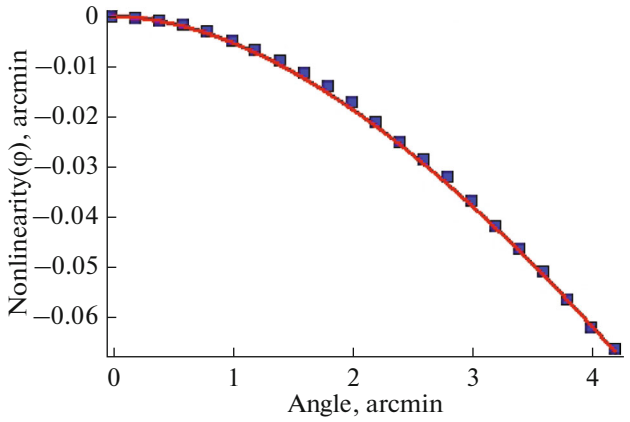

Fig. 3. Experimental dependences of resonance frequency on amplitude (blue dots) and approximation by analytical formula (9) with parameters $k_1 = 1.75 \times 10^{-4}$, $k_2 = 1.05 \times 10^{-3}$—red line.

Then, the moment of elastic force M_{flex} is defined as follows:

$$M_{\text{flex}} = -\frac{\partial U}{\partial \varphi} = -ca(\varphi)\frac{da(\varphi)}{d\varphi} \equiv -c(\varphi + \text{Nonl}(\varphi)),$$

which makes it possible to determine function Nonl(φ) using the inverse dependence $a(\varphi)$ obtained with the use of (7):

$$\text{Nonl}(\varphi) \equiv a(\varphi)\frac{da(\varphi)}{d\varphi} - \varphi. \qquad (8)$$

The results obtained in the processing of the experimental dependence $F(\nu)$ from Fig. 2 using Equations (7) and (8) are shown with blue dots in Fig. 3. Integration by formula (7) involved linear interpolation between the experimental values of $F(\nu)$ and extrapolation to zero amplitude.

Application of filter (5) for RLG real-time signal processing requires analytical parameterized approximation of the experimental dependence Nonl(φ), which was approximated in this case by the two-parameter formula (9):

$$\text{Nonl}(\varphi) = k_1\left[\text{sgn}(\varphi)\left(\sqrt{1 + \frac{|\varphi|}{k_2}} - 1\right) - \frac{\varphi}{2k_2}\right]. \qquad (9)$$

This formula provides a minimum approximation error in the range of the specified amplitudes of the sinusoidal dither as well as a satisfactory approximation error beyond the range of the specified amplitudes, which is important at pulse action on the SINS. Approximation (see Fig. 2) was performed at $k_1 = 1.75 \times 10^{-4}$, $k_2 = 1.05 \times 10^{-3}$ for angle φ in radians.

DISSIPATION OF OSCILLATION ENERGY

Physical mechanisms of the suspension oscillation energy dissipation determine the analytic formula for the term Diss(φ). Dissipation may be due to losses caused by viscous friction of the RLG ambient gas or the losses in elastic torsions of the suspension. The quality factor Q of the resonance oscillations of the RLG with a perimeter of 28 cm and a frequency of about 400 Hz due to viscosity of the ambient gas is estimated to be about 10^7, which is much higher than the experimental values of $Q \sim 10^2$.

Hence, the main mechanism of dissipation is internal friction in the material of the suspension torsions. The internal friction in solids is well understood [14–17]. Its distinguishing feature is the hysteresis nature of force-displacement relationship and independence of force from speed. As distinct from viscous friction (often called "wet"), the force of which is proportional to the speed uneven degree, loss in oscillation energy at hysteresis is proportional to the figure square in the force-displacement coordinates and does not dependent on the shape of this figure. The equation of ellipse [14–17] is convenient to use to obtain the formula:

$$\text{Diss}(\varphi) = \text{sgn}(\dot{\varphi})k_3 a(1 + k_4 a)\sqrt{1 - \frac{\varphi^2}{a^2}}. \qquad (10)$$

Parameter k_3 determines the value of the suspension vibration energy dissipation, k_4 determines the dependence of the dissipation value on the vibration amplitude.

PIEZOCERAMIC DRIVE OF THE ELASTIC SUSPENSION

The elastic suspension of the single-axis RLG is generally designed in the form of elastic torsions (an even number) that mechanically connect the glass-ceramic body of the RLG with the SINS housing. The torsions have electrically interconnected piezoceramic plates glued onto their surfaces; the plates are supplied with AC voltage V.

Under voltage V, the inverse piezoelectric effect of the piezoceramic plates causes bending deformation of the torsions, which in turn causes RLG rotation relative to the SINS.

Since the oscillations of piezoceramics are directed normally to the applied voltage, this corresponds to the piezoelectric soft mode CH_t with independent electrical variable E_x, and the equations of the state of inverse and direct piezoelectric effects have the form [18]:

$$\varepsilon_y = s_{yy}^E \sigma_y + d_{31} E_x, \qquad (11)$$

$$D_x = d_{31}\sigma_y + \varepsilon_{xx}^T E_x, \qquad (12)$$

where ε_y, σ_y are deformation and mechanical stress of the piezoceramic plate along the suspension radius, respectively: D_x, E_x are induction and intensity of the electric field in the direction perpendicular to the plate plane: d_{31} is the perpendicular piezoelectric coefficient of piezoceramics: $s_{yy}^E, \varepsilon_{xx}^T$ are the elastic coefficient and the absolute dielectric constant of piezoceramics.

Using the notation Δ, L for the thickness and height of the torsion bar, d, l—the thickness and width of the piezoelectric plate along the suspension radius, N—the number of torsions in the suspension, R_d—the suspension radius, and taking into account that $E_x = V/d$, from Equation (11) we obtain the formula for M_{piezo}:

$$M_{\text{piezo}} = -\frac{NdL\Delta^2 R_d}{s_{yy}^E l^2}(\varphi_{\text{RLG}} - \varphi_{\text{SINS}}) - \frac{NL\Delta d_{31}}{s_{yy}^E} V. \quad (13)$$

The first term in (13) describes increase in the torsional stiffness of the suspension due to the elastic properties of piezoceramics; it can be taken into account in the coefficient c of Equation (2). The second term describes the dynamic excitation of the oscillator under the applied voltage V.

The direct piezoelectric effect described by (12) determines the value of the equivalent capacitance C_0 of the suspension piezoceramics. Large values of C_0 and output resistance of the suspension drive can cause an antiresonance effect [18], when at frequencies higher than the basic mechanical resonance, the RLG oscillation amplitude decreases significantly, leading to a more balanced form of AFC. In this case, equation $E_x = V/d$, and hence Equation (13), become sufficiently approximate.

The antiresonance effect has a less impact on RLG with lower resonance frequencies of the suspension. According to the results of AFC measurements for RLGs with a perimeter of 28 cm from different manufacturers, the AFC simulation accuracy with account of only the proportional relationship between M_{piezo} and V (13) may be from a few arcsec to several tens of arcsec for different batches.

In this paper we restrict ourselves to the case when Equation (13) can be applied. The coefficient of proportionality between M_{piezo} and V contains the values of physical parameters of piezoceramics that can vary significantly with temperature and time during SINS operation. Therefore, we need to enter the parameter of dynamic excitation k_5

$$\text{Piezo}(V) = k_5 V \quad (14)$$

the value of which should be determined during SINS operation.

To obtain the relationship between the dissipation model parameter k_3 and the dynamic excitation parameter k_5 with the values determined experimentally during SINS operation, consider Equation (2) in the absence of kinematic excitation ($\varphi_{\text{SINS}} = 0$) and nonlinearity of elastic force $\text{Nonl}(\varphi)$.

Assume that at the resonance frequency the preset voltage V is given as

$$V = V_m \cos(\omega_0 t).$$

We seek the solution to $\varphi_{\text{RLG}} = a(t)\sin(\omega_0 t)$, where $a(t)$ is the function slowly varying over the period of resonance oscillations. The substitution in Equation (2) and neglect of the second derivative of $a(t)$ result in the following equation:

$$\frac{2\dot{a}}{\omega_0} = -k_3 a(1 + k_4 a) - k_5 V_m. \quad (15)$$

Taking into account the determination of the mechanical quality factor Q of the oscillatory circuit [14–17], from (15) we derive:

$$k_3(1 + k_4 a) = 1/Q. \quad (16)$$

In the conditions of stationary amplitude $\dot{a} = 0$, we obtain the formula for k_5:

$$k_5 = -a_m/(QV_m). \quad (17)$$

Equations (16), (17) allow the dissipation model parameter k_3 and the dynamic excitation parameter k_5 to be determined during the SINS operation using the value of the mechanical quality factor Q and the average value of voltage V_m applied to the elastic suspension, needed to provide the required average value of the oscillation amplitude a_m. Parameter k_4 has little effect on the simulation accuracy (see below) and can be set as a constant for a batch of elastic suspensions.

The value of the mechanical quality factor Q and coefficients k_1, k_2 can be determined in the process of SINS operation at amplitude modulation of the elastic suspension, applied to eliminate dynamic minibands of the RLG. The algorithm of this determination depends on the specific amplitude modulation algorithm, which is why it is not considered in this paper.

NUMERICAL SIMULATION AND EXPERIMENTAL VERIFICATION OF THE CORRECTING FILTER

To test the adequacy of the accepted models, we performed numerical simulations of Equation (2) under dynamic excitation and in the absence of kinematic excitation, which corresponds to four curves in Fig. 2 for the ten selected frequencies close to the resonance one. Parameters ω_0, $k_1 - k_5$ of the above models were varied to achieve the minimum of the objective function S:

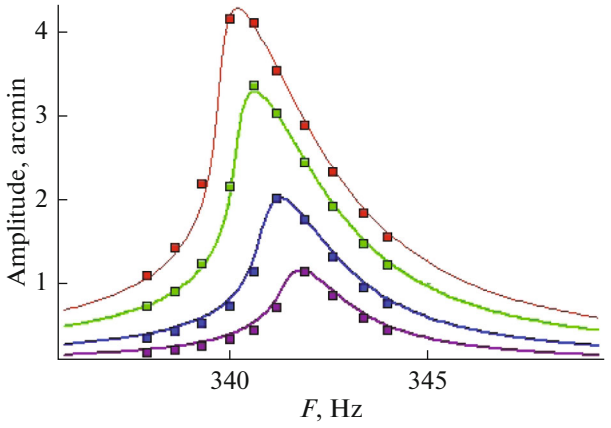

Fig. 4. Comparison of AFC simulations at k_1=1.75 × 10^{-4}, k_2 = 1.05 × 10^{-3}, k_3 = 4.4 × 10^{-3}, k_4 = 250 with the experimental data.

$$S = \frac{1}{4\times 10}\sum_{i=j=1}^{i=4,j=10}(a_{\text{model},i,j} - a_{\text{experiment},i,j})^2.$$

At its minimum, the value of S gives 4 arcsec RMS deviation of the model from the experimental one. The values of model parameters show a good qualitative and quantitative agreement between the calculated and experimental values of the oscillation amplitude (Fig. 4).

The minimum value of the objective function was used to calculate the sensitivity coefficients as the ratio of increase in the RMS error to 1% of the value of this parameter. The results are shown in the table.

Table shows that the error model is mostly affected by the resonance frequency ω_0, whereas coefficient k_4 has the least effect on it.

The study involved numerical simulation of the RLG operation in the SINS. Dynamic excitation was applied on a resonance frequency of 386 Hz at the RLG oscillation amplitude of 3 arcmin. Kinematic vibration excitation was applied to SINS with the amplitude of 1 arcmin in the frequency range of 80–3600 Hz. The simulated RLG signal output was fed with a frequency of 7.2 kHz both to the input of a 10th-order elliptic IIR eliminator with a 370–410 Hz suppression frequency band [3, 9, 19] and to the input of the digital correcting filter (5).

The simulation results are presented in Fig. 5. It can be seen that the eliminator suppresses the mechanical dither frequency successfully, but, at the same time, it does not pass the useful SINS signal of

Sensitivity coefficients of the model, arcmin/%

ω_0	k_1	k_2	k_3	k_4	k_5
2.65	1.05 × 10^{-2}	1.9 × 10^{-2}	1.0 × 10^{-2}	2 × 10^{-3}	1.7 × 10^{-2}

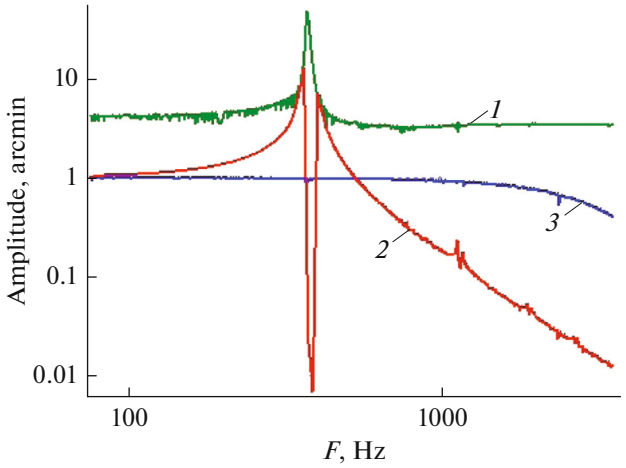

Fig. 5. Calculated frequency dependence of the single-axis RLG at dither oscillation amplitude of 3 arcsec (curve *1*); calculated frequency dependence for the 10th-order digital elliptic eliminator (curve *2*), and digital correction filter (curve *3*).

1 arcmin. We see the AFC rise near the resonance frequency due to the mechanical resonance of the elastic suspension. Above 500 Hz, there is a roll-off with a slope of 6 dB /octave, which is due to the roll-off of the mechanical filter AFC.

In general, the frequency response of the eliminator shows passband ripple, and the mechanical dither passband is limited.

The correcting digital filter shows much smoother AFC with the exception for the range of frequencies close to the Nyquist frequency (see Fig. 1). To improve the smoothness of the correcting digital filter, the sampling rate must be chosen with a reserve.

Note that the eliminator described in [7, 8] does not provide uniform AFC on moving averages in the desired bandwidth either, because, as with the elliptic filter, it does not account for the AFC roll-off with a slope of 6 dB/octave above the resonance frequency.

To experimentally test the correcting filter, we used SINS with an RLG with a perimeter of 28 cm. The inertial measurement unit was fixed rigidly (without any shock absorbers) to the SINS base. The analog beat-frequency signal was digitized at a frequency of 72 kHz by the dual comparator and a dual 12-bit AD converter. Digital values from the comparator and the AD converter were combined into two integers by the digital signal processor. To reduce the noise, digitized values were passed through a low pass filter with a 9 kHz bandwidth and then decimated to the frequency of 7.2 kHz.

Coefficients $k_1 - k_3$ and the quality factor Q were estimated by a digital signal processor during SINS operation, based on the results of amplitude modulation of the dither in order to eliminate dynamic minizones of the RLG. k_5 was determined by a system of

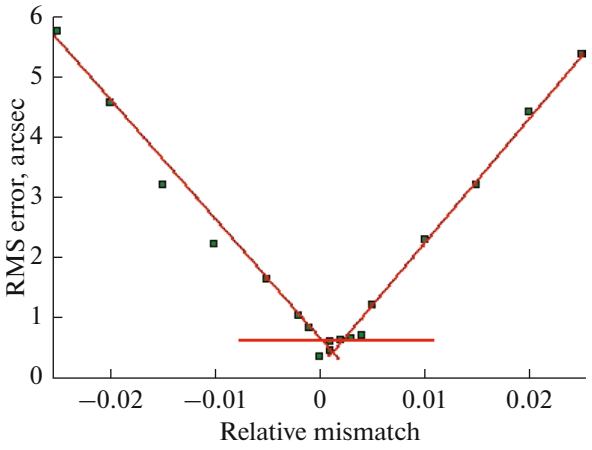

Fig. 6. Experimental dependence of the RMS error of dither signal suppression by the correcting filter for a stationary SINS.

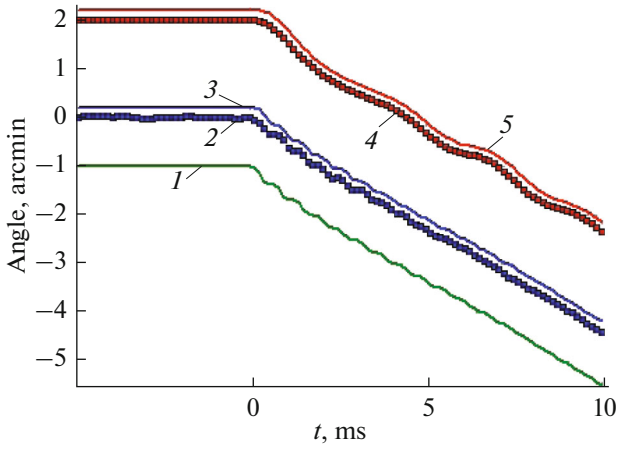

Fig. 7. The experimental (curves *2* and *4*) and calculated (curves *3*, *5*) dependences of SINS position under the impact. Curves *4*, *5* correspond to the 10th order elliptic eliminator, curves 2 and *3*, to the correcting filter, curve *1*, to the simulated simulation rotation. The curves are shifted vertically for illustration purposes.

amplitude stabilization from the known average values of amplitude and voltage a_m, V_m; due to the low sensitivity value (see Table), k_4 was set a constant. Resonant frequency ω_0 was determined by the dither phase-locked loop taking into account a relative mismatch at known coefficients k_1, k_2, and a_m.

The quality of suppression of the dither signal by the digital correcting filter was tested in the first experiment. The SINS was stationary relative to the Earth. After the correcting filter the digital signal was recorded with a frequency of 7.2 kHz in the software buffer during 4 oscillation periods of the dither. The dither dynamic excitation amplitude was 3 arcmin. The resonance frequency was 386 Hz.

The signal RMS error was calculated from its average value. Frequency mismatch ω_0 of the filter (5) operation with vibrodrive operation frequency was previously programmed. From Fig. 2 it is clear that due to the vibrodrive nonlinearity, frequency ω_0 must be above the resonance frequency. For complete suppression, the calculated value of the relative mismatch was 0.0025. The measurement results are given in Fig. 6.

It is seen that when relative mismatch is about 0.002, which is close to the calculated value, the RMS error is at its minimum, about 0.7 arcsec.

The second experiment was aimed at estimating the adequacy of the simulated AFCs of the correcting filter and elliptic eliminator (Fig. 5). The SINS was mounted on the platform allowing for single-axis rotation in the sensitivity axis of the RLG being tested. The stationary platform was hit tangentially with a metal striker, which caused SINS rotation. A wide spectrum of SINS rotation at the moment of impact made it possible to estimate the AFC ripple of the filters.

The RLG output signal in one decimation cycle was processed through the correcting filter and elliptic eliminator. The program detector of the impact recorded the filtering results into two memory buffers simultaneously. The experimental data are shown in Fig. 7 by the curves: *2*—for the correcting filter and *4*—for the elliptic eliminator.

For the elliptic eliminator, after the impact at time point $t = 0$ ms, we can see an oscillatory response with a period of about 2 msec, which is in close agreement with the calculated AFC with rises during the mechanical resonance of the dither (see Fig. 5). On the contrary, the correcting filter shows an abrupt start of motion, which can be indicative of a broad bandwidth and flat AFC.

Since the actual SINS rotation, common to the both filters, after the impact was unknown, we performed mathematical variation of the simulated rotation (Fig. 7, curve *1*) and postprocessing by the both filters to minimize the differences between the results of the simulated (Fig. 7, curves *3* and *5*) and actual (curves *2* and *4*) data. The simulated rotation contained an oscillating decaying component with a frequency of about 1.6 kHz, which was most probably caused by the mechanical vibration of the SINS after the impact. We can see qualitative and quantitative agreement of the results obtained for the both filters in the simulation and the results of the real SINS rotation. The eliminator output does not have an oscillating component at a frequency of 1.6 kHz because the bandwidth is limited by the resonance frequency of the vibrodrive. We can also see a good agreement between the experimental curve *2* obtained with the correcting filter and the optimal simulated rotation (curve *1*). This may mean that the correcting filter, in contrast to

the elliptic eliminator is much more accurate in restoring the actual rotation of the SINS, which is necessary for navigation algorithms.

According to the results of the numerical calculations and the experiments described above it may be concluded that the correcting digital filter shows satisfactory operation at zero frequency (absence of rotation) and at broadband rotation (mechanical impact).

CONCLUSIONS

A correcting digital filter has been proposed to determine the angular position of SINS in the sensitivity axis of the single-axis mechanically dithered RLG. The SINS angular position is determined by the known value of the RLG angular position with respect to the inertial space taking into account the models of the suspension elastic forces nonlinearity, the hysteresis model of oscillation energy dissipation, and the model of the suspension piezoceramic drive.

Parameterized models of nonlinearity, dissipation and output characteristics of the elastic suspension piezodrive have been developed.

The numerical simulations of AFCs of the elliptic eliminator and correcting filter under SINS sinusoidal rotation with the amplitude of 1 arc min over the frequency range of 80 to 3600 Hz have shown that unlike the correcting filter, the eliminator has a significant AFC ripple.

The experimental results show that in the absence of SINS rotation, the correcting filter is capable of eliminating mechanical dither from the RLG signal.

The experimental verification of the efficiency of the proposed correcting filter at pulse action on SINS has confirmed the adequacy of the proposed models and satisfactory operation of the correcting digital filter.

REFERENCES

1. Aronowitz, F., Fundamentals of the ring laser gyro. *Optical Gyros and their Application (RTO AGARDograph 339*, 1999, p. 3-1–3-45).
2. Anuchin, O.A. and Emelyantsev, G.I., *Integrirovannye sistemy orientatsii i navigatsii dlya morskikh podvizhnukh ob"ektov* (Integrated Navigation and Orientation Systems for Marine Vehicles), Peshekhonov, V.G., Ed., St. Petersburg: CSRI Elektropribor, 2003.
3. Kuznetsov, A.G., Molchanov, A.V., Chirkin, M.V., and Izmailov, E.A., Precision laser gyro inertial navigation for autonomous, *Kvantovaya elektronika*, 2015, vol. 45, no. 1, pp. 78–88.
4. Wang Kedong and Gu Qitai, Key problems of mechanically dithered system of RLG, *Tsinghua Science and Technology*, 2001, vol. 6, no. 4, pp. 304–309.
5. Hemalatha, N., Chandrasekhar, R.S, Bai A. Swarna, and Reddy G. Satheesh, A linear observer design for dither removal in ring laser gyroscopes, *IFAC, Embedded Guidance, Navigation and Control in Aerospace*, 2012, vol. 1, Part 1, pp. 63–66.
6. Banerjee, K., Dam, B., Majumdar, K., Banerjee, R., and Patranabis, D., An improved dither stripping scheme for strap down ring laser gyroscopes, *TENCON 2004 Conference of IEEE*, vol. 1, pp. 689–692.
7. Enin, V.N. and Saneev, V.I. Digital oscillator for dither of the laser gyro. *Nauka i Obrazovanie*: *nauchnoe izdanie MGTU im. N.E Baumana,* 2015, no. 05, pp. 154–177.
8. Enin, V.N., Lyudomirskii, M.B., and Saneev, V.I., Influence of output resolution of the pulse-phase detector of the laser gyro on measurement accuracy of small angular rates, *Inzhenernyi vestnik*, 2013, no. 11, pp. 609–624.
9. Molchanov, A.V., Belokurov, V.A., Chirkin, M.V., Koshelev, V.I., Mishin, V.Yu., and Morozov, D.A., Precision laser gyroscope with a digital channel for quadrature signal processing, *22nd St. Petersburg International Conference on Integrated Navigation Systems*, St. Petersburg: Elektropribor, 2015, pp. 307–314.
10. Salychev, O.S. *Applied Inertial Navigation: Problems and Solutions,* Moscow: BMSTU Press, 2004.
11. Il'in, M.M., Kolesnikov, K.S., and Saratov, Yu.S., *Teoriya Kolebanii* (Theory of Oscillations, Moscow: MGTU im. Baumana, 2003.
12. Ifeachor, E.C. and Jervis, B.W., *Digital Signal Processing: A Practical Application, 2nd addition*, Pearson Education, Harlow, UK, 2002.
13. Landau, L.D. and Lifshits E.M., *Mekhanika* (Mechanics), Moscow: Nauka, 1988.
14. Panovko, Ya.G., *Vnutrennee trenie pri kolebaniyakh uprugikh system* (Internal Friction at Vibration of Elastic System), Moscow: Fizmatlit, 1960.
15. Panovko, Ya.G., *Vvedenie v teoriyu mekhanicheskikh kolebanii* (Introduction to the Theory of Oscillation), Moscow: Fizmatlit, 1989.
16. Pisarenko, G.S., *Kolebaniya mekhanicheskikh sistem s uchetom nesovershennoi uprugosti materiala* (Vibration of Mechanical Systems with Consideration for Imperfect Elasticity of the Material), Kiev: Naukova dumka, 1970.
17. Zoteev, V.E., *Parametricheskaya identifikatsiya dissipativnykh mekhanicheskikh sistem na osnove raznostnykh uravnenii* (Parametric Identification of Dissipative Mechanical Systems based on Difference Equations), Radchenko, V.P., Ed., Moscow: Mashinostroenie, 2009.
18. *P'ezokeramicheskie preobrazovateli. Metody izmereniya i raschet parametrov. Spravochnik*. (Piezoceramic Transducers. Methods of Measurement and Calculation of Parameters. Handbook.) Pugachev, S.I., Ed., Leningrad: Sudostroenie, 1984.
19. Lutovac, M.D., Tosic, D.V., and Evans, B.L., *Filter Design for Signal Processing using MATLAB and Mathematica*, NJ, USA: Prentice Hall, 2001.